



Received: 03 September, 2025
Accepted: 10 September, 2025
Published: 11 September, 2025

***Corresponding author:** Bao Lei, School of Architectural Engineering, Tianjin University, Tianjin 300350, China, E-mail: lbao@tju.edu.cn

Keywords: Organics; Chemical phosphorus removal; Hydroxyl oxide; Carboxyl group

Copyright License: © 2025 Xinsheng L, et al. This is an open-access article distributed under the terms of the Creative Commons Attribution License, which permits unrestricted use, distribution, and reproduction in any medium, provided the original author and source are credited.

<https://www.engineergroup.us>



Research Article

Effect of Different Organic Compounds on Phosphorus Removal by Ferric Iron-dependent in Wastewater Treatment

Lu Xinsheng¹, Zhao Zhiguo^{2,3}, Wang Wenyan², Bao Lei^{4*}, Cao Qixin¹, Yang Xian^{3*}, Tan Huan², Lai Linlin³, Liu Mengyu⁵, Yang Fugang^{2,3}, Li Yong² and Li Diandian⁶

¹PowerChina Northwest Engineering Corporation Limited, Xi'an 710065, China

²Shaanxi Metallurgical Design and Research Institute, Xi'an 710055, China

³School of Environmental and Municipal Engineering, Xi'an University of Architecture and Technology, Xi'an, 710055, PR China

⁴School of Architectural Engineering, Tianjin University, Tianjin 300350, China

⁵School of Biological and Environmental Engineering, Xi'an University, Xi'an 710055, China

⁶China Datang Corporation Science and Technology General Research Institute Co., LTD Northwest Branch, Xi'an, 710055, China

Abstract

The iron ion (Fe(III)-dependent phosphorus removal process) is frequently observed to be inefficient in current wastewater treatment technologies, particularly in the presence of organic compounds in the wastewater. However, the precise mechanism by which this occurs remains unclear. In this study, the effects of different organic compounds, including citric acid, xanthate, polysorbate 80, bovine serum albumin, glucose, and starch, on the efficiency of Fe(III)-dependent phosphorus removal were investigated in depth through the use of well-designed batch experiments combined with the analytical techniques of Fourier Transform Infrared Spectroscopy (FTIR) and X-ray Diffraction (XRD). The experimental results yielded a significant finding: carboxylic organics, particularly polycarboxylic organics such as citric acid, exerted a markedly greater influence on phosphorus removal efficiency than hydroxy organics, exhibiting an intensity index as high as 5 to 20 times that of other organics. Specifically, citric acid was observed to reduce the number of binding sites available for phosphate, competing with phosphate for the surface binding sites of iron hydroxyl oxides (Fe-HFOs). This resulted in a significant reduction in phosphorus removal efficiency. Furthermore, this study presents an innovative mechanistic model to elucidate the mechanism by which organic matter "seizes" the surface of Fe-HFO, leading to the reduction of phosphorus removal efficiency. This study not only enriches the theoretical basis of chemical phosphorus removal but also provides new perspectives and technical support for the pretreatment of organic matter in practical wastewater treatment. This is of great theoretical and practical significance for improving the efficiency of wastewater treatment in the future.

Introduction

Chemical agents, including ferric iron (Fe(III)), were introduced into wastewater with the objective of precipitating phosphate for the purpose of wastewater treatment, a process that has been identified as chemical phosphorus removal [1-3]. In recent years, chemical phosphorus removal has been widely adopted in wastewater treatment plants (WWTP) due to its convenient operational characteristics, straightforward

regulatory requirements, and minimal secondary pollution [4-6]. It has been postulated by numerous researchers that the formation of $\text{Fe}_2(\text{PO}_4)_3$ and FeP mineral variants is responsible for the Fe(III)-dependent phosphorus removal [7-9]. In contrast, Galarneau, et al. [10] proposed that the removal of phosphorus was due to the generation of hydroxyl oxide (Fe-HFO) by Fe(III), which then adsorbed phosphate and facilitated its removal. Models developed by Smith and Hauduc, et al. demonstrated that the adsorption of phosphate to Fe-HFO,

rather than the formation of $\text{Fe}_2(\text{PO}_4)_3$ precipitation, was the primary mechanism responsible for the removal of phosphate by Fe(III) [11,12]. Furthermore, Antelo, et al. observed that the binding of phosphate to goethite was robust [13]. Nevertheless, a definitive conclusion regarding the mechanism of Fe(III)-dependent phosphorus removal remains elusive. As indicated in the literature, a multitude of factors, including the quantity of reagent, pH value, temperature, hydraulic condition, impurity, and others, have the potential to impact the efficacy of Fe(III)-dependent phosphorus removal [14]. An increasing number of studies have been conducted to investigate the impact of diverse substances on chemical phosphorus removal processes. Among these factors, the influence of organics is relatively complex, as they affect both the thermodynamics and kinetics of coagulation reactions. The influence of organics on coagulation remains unclear due to the diverse range of organic substances present in water. The investigation of the impact of organics on chemical phosphorus removal is of paramount importance, as it not only facilitates a comprehensive understanding of this process but also offers valuable insights into the mechanisms governing coagulation.

Among the plethora of organic compounds present in wastewater, Citric Acid (CA) is one of the most abundant [23]. Citric Acid (CA) is a widely utilized chemical in numerous industries, and it is an indispensable organic compound in the tricarboxylic acid (TCA) cycle within living organisms. Citric Acid (CA) is a common constituent of domestic wastewater. Borggaard, et al. [25] have demonstrated that carboxyl-containing substances can influence the adsorption of phosphate. In a study by Geelhoed and colleagues, it was observed that there was a considerable degree of competition between Humic Acid (HA) and anions such as phosphate in chemical reactions. Sibanda, et al. observed that HA in soil would compete with phosphate for adsorption sites on goethite, resulting in a reduction in phosphate adsorption on Fe-HFO [30–32]. In contrast, Borggaard observed that HA had no discernible impact on the adsorption of phosphate by aluminum chloride goethite. The current state of research on the removal of phosphate by organics is still incomplete. The impact of diverse organics on the phosphorus removal process remains unclear, as does the underlying mechanism. It is therefore of considerable significance to elucidate the impact and the underlying mechanisms of organic compounds on the efficiency of Fe(III)-dependent phosphorus removal in wastewater treatment.

The efficiency of iron-ion-dependent phosphorus removal is currently affected by a variety of factors, with the organic matter in the wastewater representing a significant influence. While studies have been conducted to investigate the effects of specific organics on phosphorus removal, these studies are often limited to laboratory conditions and thus lack the comprehensive scope necessary to consider the full range of organic species and concentrations. Moreover, further research is required to elucidate the specific mechanisms of interaction between iron ions and organic matter, as well as to optimize the use of iron ions in practical wastewater treatment, with the aim of improving phosphorus removal efficiency and reducing the negative effects of organic matter.

To address the aforementioned issues, this study systematically compared the effects of different organic compounds on Fe(III)-based phosphorus removal and identified carboxyl groups as the key factor governing interference intensity. Batch experiments demonstrated that carboxylic acids, particularly citric acid, inhibit phosphorus removal far more strongly than hydroxyl-based organics. To quantitatively assess this effect, we introduced an “impact intensity index,” which provides the first standardized metric for comparing the inhibitory strength of different organics. Fourier Transform Infrared Spectroscopy (FTIR) and X-ray Diffraction (XRD) analyses further revealed that carboxyl groups compete with phosphate for surface binding sites, forming stable organic-iron complexes that suppress phosphorus removal. These findings establish both a quantitative framework and a mechanistic model for organic interference, offering theoretical and technical guidance for optimizing wastewater treatment.

Materials and methods

Materials

Instruments: The following instruments were utilized in this study: an X-ray diffractometer from Ultiman IV (Japan), a Fourier infrared spectrometer (United States, Nicolet iS50), an electronic balance (German, Dolly BSA224S), a ultraviolet spectrophotometer (UV2600), a coagulation six league mixer (MY30000–6 g), a centrifuge table low speed (Shanghai Anting TDL–4DB), a Zeta voltmeter (ZS90Zeta, Melvin, UK), and a pH meter (Ray magnetic PHS–3E).

The following agents were utilized: iron hexahydrate chloride, anhydrous sodium acetate, anhydrous calcium chloride, ammonium chloride, magnesium sulfate, sodium chloride, potassium dihydrogen phosphate, sodium hydroxide, hydrochloric acid, ascorbic acid, ammonium molybdate, CA, and morpholine ethyl sulfonic acid (MES). The solutions utilized in the experimental procedure were prepared with high-purity reagents and deionized water.

Synthetic wastewater: anhydrous sodium acetate (0.513 g/L), ammonium chloride (0.153 g/L), magnesium sulfate (0.154 g/L), calcium chloride (0.042 g/L). In accordance with the experimental design, potassium dihydrogen phosphate, iron hexahydrate chloride, and organics were added as required in different experiments.

Methods

The pH is a significant factor influencing the efficiency of phosphorus removal by Fe(III). Accordingly, the pH value in the reaction system was calibrated to 7 ± 0.2 with 10 mmol·L⁻¹ morpholine ethyl sulfonic acid (MES) buffer [34]. The reaction system was supplemented with 0.1 mmol·L⁻¹ NaCl to ensure a constant ionic strength in the solution.

Experiment on effects of organics on phosphorus removal: The typical organics were selected based on the analysis of the wastewater contents, which revealed the presence of starch, glucose, bovine serum protein, Tween 80, fulvic acid (FA), and CA. The impact of varying concentrations of organics

on phosphorus removal efficiency by Fe(III) was examined through the implementation of batch tests. The concentrations of the organics were set at 0, 10, 20, 40, 80, and 100 mg·L⁻¹, respectively. The phosphorus concentration was set at 10 mg·L⁻¹, and Fe (III) was added in a ratio of n (Fe): n (P) = 1.4:1. The beaker containing the synthetic wastewater was placed in a six-link mixer and subjected to agitation at 200 rpm for one minute and 50 rpm for 15 minutes. Subsequently, the beaker was allowed to stand for 20 minutes. Samples were collected from a depth of 2 to 3 cm below the liquid surface to determine the concentration of dissolved phosphorus.

Comparison of phosphorus removal methods: In order to investigate the phosphorus removal process of iron salt, two distinct groups were established: the conventional chemical phosphorus removal group (CCPR group) and the iron hydroxyl oxide (Fe-HFO) phosphorus removal group.

The CCPR group is defined as follows: Subsequently, Fe (III) (25.3 mg·L⁻¹) and CA (0–30 mg·L⁻¹) were added in a sequential manner to an aqueous solution with a phosphorus concentration of 10 mg·L⁻¹. The alteration of the chemical bond in the sediments before and following the addition of CA was ascertained through FTIR analysis. X-ray diffraction (XRD) spectroscopy was employed to ascertain the alteration in the composition of the sediments before and following the introduction of CA.

The HFO group prepared a solution of Fe-HFO according to the methodology outlined in the published source [35]. Subsequently, phosphate (10 mg·L⁻¹) and CA (0–30 mg·L⁻¹) were added successively to the Fe-HFO solution (25.3 mg·L⁻¹). Periodic samples were obtained for the purpose of determining the efficiency of phosphate removal in both systems. The alteration of the chemical bond in the sediments before and following the addition of CA was ascertained through FTIR analysis. The alteration in the material composition of the sediments before and following the introduction of CA was ascertained through XRD spectroscopy.

FTIR and XRD spectroscopy detection: The Fourier transform infrared spectroscopy (FTIR) was employed to investigate the formation and fracture of chemical bonds during the Fe(III)-dependent phosphorus removal process. X-ray diffraction spectroscopy was employed to ascertain the nature of the products formed during the Fe(III)-dependent phosphorus removal process. The phosphorus removal products described in section 1.2.2 were collected, washed, centrifuged, and allowed to dry naturally. They were then analyzed by FTIR and XRD spectroscopy. All samples were subjected to analysis on the platform of the Shaanxi Provincial Key Laboratory of Environmental Engineering.

The XRD data analysis revealed that the diffraction angle, intensity, and crystal plane spacing of the 20–0011 diffraction peak were consistent with the data of the standard card (lepidocrocite: JCPDS no. 74–1877, goethite: JCPDS no. 81–0464) in the Joint Committee on Powder Diffraction Standards (JCPDS) database.

Results and discussion

The organic matter concentrations applied in this study (0–160 mg·L⁻¹) were designed to reflect typical wastewater conditions, ensuring that the observed removal patterns can be directly linked to the Dissolved Organic Carbon (DOC) and Volatile Fatty Acid (VFA) profiles of real systems, thereby enhancing the engineering relevance of the findings.

Citric acid (0–100 mg·L⁻¹) and fulvic acid (0–160 mg·L⁻¹) were selected to encompass representative conditions of municipal sewage (DOC 10–50 mg·L⁻¹, with VFAs contributing 20–40% or 5–20 mg·L⁻¹) and industrial wastewater (DOC 50–150 mg·L⁻¹, VFA >50% of DOC; up to 80–120 mg·L⁻¹ in citric acid production effluents). For example, 20 mg·L⁻¹ citric acid reduced phosphorus removal efficiency by ~30%, consistent with fluctuations observed in municipal sewage during high-VFA periods (15–25 mg·L⁻¹ in early rainy seasons). At 80 mg·L⁻¹ citric acid, removal efficiency declined by >70%, mirroring challenges in untreated food-processing wastewater. These outcomes validate the practical representativeness of the experimental design.

A clear relationship was established between phosphorus removal inhibition and the proportion of carboxyl functional groups. When carboxyl-containing organics constituted <30% of DOC (as in municipal sewage), efficiency loss was <20% even at DOC levels of 40 mg·L⁻¹ (e.g., 20 mg·L⁻¹ furfural acid with 0.75 carboxyl groups). In contrast, when carboxyl organics exceeded 50% of DOC (typical of industrial effluents), only 60 mg·L⁻¹ DOC was sufficient to cause >50% efficiency loss (e.g., 60 mg·L⁻¹ citric acid with a carboxyl content of 1.56). These patterns provide actionable engineering guidance: in municipal wastewater, phosphorus removal remains stable if VFA/DOC <0.3, or aerobic stripping reduces VFA to <20 mg·L⁻¹; in high-carboxyl industrial wastewater, pretreatments such as anaerobic digestion or Ca²⁺ addition should limit carboxyl organic concentrations below 40 mg·L⁻¹ to maintain Fe(III)-based removal efficiency above 80%.

In summary, the experimental concentration gradient aligns well with real DOC/VFA distributions, allowing removal rate patterns to be directly mapped to engineering contexts. This provides a robust quantitative basis for optimizing pretreatment strategies in municipal and industrial wastewater, significantly enhancing the practical applicability of the conclusions.

Effects of organics on ferric ion-dependent phosphorus removal

Figure 1 illustrates the impact of various chemical and biological agents, including CA, FA, polysorbate-80, bovine serum protein, glucose, and starch, on the efficiency of phosphorus removal when Fe (III) is employed as a flocculant. Upon increasing the concentration of starch and glucose in the reaction system from 0 mg·L⁻¹ to 160 mg·L⁻¹, the amount of phosphorus removed remained relatively constant. As the concentration of bovine serum protein, polysorbate-80, FA, and CA increased from 0 mg·L⁻¹ to 160 mg·L⁻¹, the phosphorus

removal percentage of the reaction system exhibited a decline in conjunction with the rise in organic concentration.

For the sake of convenience in analysis, the decreased phosphorus removal percentage per $\text{mg}\cdot\text{L}^{-1}$ of organics was defined as the influence intensity index of the specified organic. The original index based on mass concentration ($\text{mg}\cdot\text{L}^{-1}$) was reformulated on a molar basis, defined as “the percentage decrease in phosphorus removal efficiency per $\text{mmol}\cdot\text{L}^{-1}$ of organic matter (or per $\text{mmol}\cdot\text{L}^{-1}$ of carboxyl functional groups).” This normalization eliminates bias arising from differences in molecular weight among organic compounds and more accurately captures the relationship between chemical characteristics (e.g., carboxyl group content) and phosphorus removal interference. For instance, at equal mass concentrations, citric acid (3 carboxyl groups, $192\text{ g}\cdot\text{mol}^{-1}$) and fulvic acid (average 1.5 carboxyl groups, $\sim 500\text{ g}\cdot\text{mol}^{-1}$) yield markedly different carboxyl molar concentrations. Thus, a carboxyl molar-based index more objectively reflects the true functional group activity. By employing a linear fitting technique to analyze the declining trend observed in each of the six selected organic lines presented in Figure 1, the resulting influence intensity indexes are presented in Table 1. The CA exhibited the greatest influence intensity index among the selected organics. It was observed to be 5 to 20 times higher than the other organics.

All six of the selected organics contain both a hydroxyl group and a carboxyl group. The ratios of hydroxyl and carboxyl functional groups in each organic are also presented in Table 1. Starch and glucose are notable for their abundance of hydroxyl groups. With regard to the impact of starch and glucose on Fe(III)-dependent phosphorus removal (Figure 1),

the hydroxyl group was found to exert no discernible influence on the efficiency of phosphorus removal in the presence of Fe(III) as flocculants. Upon alteration of the concentrations of the organics, the removal percentages of phosphate exhibited a maximum decline of 15.11% (starch) and 16.28% (glucose). This finding suggests that the hydroxyl group exerted minimal influence on the Fe(III)-dependent phosphorus removal efficiency, a conclusion that aligns with the observations documented by Hue, et al. [36,37].

It is widely known that bovine serum protein contains a multitude of amino acid residues, that polysorbate-80 contains unsaturated fatty acids, and that FA contains carboxyl, hydroxyl, and other functional groups. As illustrated in Figure 1, these three organics exerted a notable influence on the Fe(III)-dependent phosphorus removal efficiency. The maximum decrease in phosphorus removal percentage was observed with bovine serum protein (43.02%), polysorbate-80 (36.05%), and FA (43.02%). Both bovine serum protein and FA contain a small quantity of carboxyl groups, whereas polysorbate-80 contains a substantial number of hydroxyl groups. The data indicate that CA has the most significant influence on the phosphorus removal efficiency when Fe(III) is used as the flocculant. The decline in phosphorus removal efficiency reached as high as 90.70%. The presence of numerous carboxyl groups in CA suggests that the carboxyl group content of organics is a crucial factor influencing their impact on Fe(III)-dependent phosphorus removal efficiency.

Further investigation is required to elucidate the mechanism by which the carboxyl group affects the Fe(III)-dependent phosphorus removal efficiency. Given its highest influence intensity index, the CA was selected as the representative organic in the following experiments to elucidate the relevant mechanism. This was achieved by detecting the formation and fracture of chemical bonds and analyzing the products in the reaction systems.

Influence of organic matter properties on the effectiveness of chemical phosphorus removal

In this experiment, three experimental groups (A, B, C) and one control group (CK) were established, with two replicates in each group.

Experimental Group A: Take one litre of effluent from the aerobic tank at the sewage treatment plant, add potassium dihydrogen phosphate, mix thoroughly, and then leave the solution to be used at a later point in time. The organic matter in the experimental system of this group is composed of particles, colloids, and ions.

Experimental Group B: The effluent from the aerobic tank of the wastewater treatment plant was allowed to stand for 12 hours, after which 1 L of the supernatant was taken, mixed well, and left for use. The organic matter in this experimental system is composed of colloids and ions.

The third experimental group is designated as Group C. The effluent from the aerobic tank of the wastewater treatment plant should be filtered through a 0.45-micron membrane.

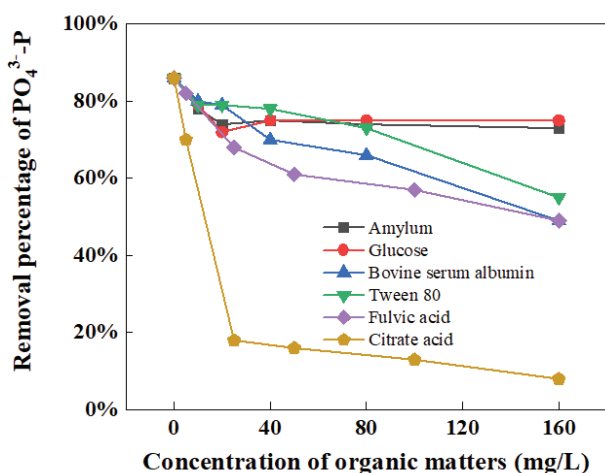


Figure 1: Effects of organics on ferric ion-dependent phosphorus removal efficiency.

Table 1: Influence intensity of different organics on phosphorus removal efficiency by iron salt.

Organic species	Starch	Glucose	BSA	Polysorbate -80	FA	CA
Influence intensity index	0.06	0.07	0.21	0.17	0.21	3.4
Carboxy number	0	0	0.49	0	0.75	1.56
Hydroxyl value	2.8	2.8	0	65-80	0.5-0.75	0.52

The resulting filtrate should be transferred to a 1-L container and stirred thoroughly before use. The organic matter in this experimental system is solely composed of ions.

The control group (CK) was prepared by taking the effluent from the aerobic tank of the wastewater treatment plant and treating it with H_2O_2 -UV until no organic matter remained. Then, 1 L of the resulting filtrate was taken, mixed well, and left to be used. The experimental system of this group is devoid of any organic matter.

1. Three hundred milliliters of the pretreated sample were placed in a beaker, which was then placed on a six-unit mixer. Subsequently, ferric chloride was added, maintaining an iron-to-phosphorus ratio of 1.4:1.
2. The indicators of each experimental system were established at the outset of the experiment.
3. The stirrer was operated as follows: The speed of the agitator was set to 300 rpm for one minute, then reduced to 50 rpm for 15 minutes.
4. Following the stirring process, the beaker was permitted to rest for a period of 20 minutes, after which the supernatant was collected for the purpose of determining the indicators.

As can be seen from the Table 2, it can be concluded that:

1. The discrepancy between the precipitated and filtered effluent in terms of iron removal is not substantial, suggesting that colloids exert minimal influence on phosphorus removal. The removal of phosphorus was found to be significantly influenced by dissolved substances and insoluble particles, with a percentage impact of 5.3% and 3.6%, respectively.
2. The alteration in pH resulting from different pretreatment water quality is not significant. Furthermore, the pH change before and after the removal of phosphorus is not considerable. However, there is a notable reduction in pH overall following the removal of phosphorus, which can be attributed to the hydrolysis of iron.
3. The ORP of the different pretreatment water qualities varies. The precipitation of sewage has the lowest ORP, while the filtration of sewage has the highest. This is due to the precipitation of sewage entering the aerobic tank, resulting in a gradual reduction in redox potential. Conversely, the filtration of sewage through the filtration of air increases the ORP.
4. The iron content of the various pretreatment samples differs significantly, with the iron content of the samples after phosphorus removal being largely consistent.
5. ZATA fluctuates at different times, but its impact on phosphorus removal is not consistent.

Table 2: The influence of different wastewater on the concentration of each pollutant under different treatment conditions.

		Raw Aerobic Tank Water	alluvial water	filtered water	Filtration + light + hydrogen peroxide
PH	pre-phosphate	7.18	7.4	7.64	7.95
	after-phosphate	7.25	7.3	7.3	7.56
ORP(mv)	pre-phosphate	36.7	10	154	210.3
	after-phosphate	59.5	170.8	159.7	280
COD(mg/L)	pre-phosphate	189	52	38	30
	after-phosphate	32	32	20	16
ZATA(mv)	pre-phosphate	-20.1	-15.1	-11.4	-11.1
	after-phosphate	-13.5	-14.3	-17	-16.5
Iron Content(mg/L)	pre-phosphate	3.5	3	0.5	0.17
	after-phosphate	0.88	0.72	0.79	0.76
Phosphorus Content(mg/L)	pre-phosphate	9.1	10.3	9.4	9.6
	after-phosphate	4.6	4.9	4.7	4.1
Fe:P Ratio		1.54	1.36	1.49	1.46
Phosphorus Removal Rate		48.80%	52.40%	52%	57.30%

Study of phosphorus remover injection and simulated domestic wastewater

In this experiment, three experimental groups (A, B, C) and one control group (CK) were established, with six replicates in each group.

Experimental Group A: Take 1.5 L of aerobic tank effluent from the sewage plant, mix it thoroughly, and allow it to be used. The organic matter in the experimental system of this group is composed of particles, colloids, and ionic organic matter, predominantly small molecules of organic matter with a high dissolved oxygen content.

Experimental Group B: Take 1.5 L of anaerobic tank water from the sewage plant, mix well, and await further instructions. The organic matter in the experimental system of this group is primarily colloidal and ionic, comprising predominantly macromolecular organic matter with no discernible dissolved oxygen.

Experimental Group C: The water from the secondary sedimentation tank of the sewage plant was collected, 1.5 L of filtrate was obtained, and the solution was stirred thoroughly and allowed to stand for future use. The organic matter in this experimental system is composed exclusively of ions. The organic matter content is minimal, as is the dissolved oxygen content.

The control group, designated CK, was configured with 1.5 L of simulated domestic sewage, which was then mixed thoroughly and prepared for use. The experimental system in this group contains dissolved organic matter and a single type of organic matter.

1. A total of 300 mL of pre-treated samples were transferred to a beaker, which was then placed on a six-mixer apparatus. Subsequently, ferric chloride was added to the beaker, with the iron and phosphorus ratio set at varying gradients.

2. At the outset of the experiment, ascertain the indicators of each experimental system.
3. The mixer was operated in accordance with the following procedure: The apparatus was set to rotate at 300 rpm for one minute and then at 50 rpm for 15 minutes.
4. Following the stirring process, the beaker was left to stand for a period of 20 minutes, after which the supernatant was extracted for the purpose of determining the indicators.

The initial water quality indicators were as follows (Tables 3-7), (Figure 2):

In conjunction with the aforementioned figure and the results presented in Table 2.1, it can be concluded that a variety of water quality parameters can be obtained. It is noteworthy that the initial pH difference is not approximately 7-7.2. Following the addition of phosphorus removal chemicals, the pH of the simulated sewage exhibited a maximum change of 5.8-6.3. Additionally, minimal alterations were observed in the remaining water quality parameters. Moreover, it can be observed that as the dosage of the drug is increased, there is a gradual decrease in pH (Figure 3).

A combination of the aforementioned graph and Table 2.1 reveals an absence of a notable correlation between ZATA and iron dosing (Figure 4).

When the aforementioned figure and Table 2.1 are considered together, it becomes evident that the simulated domestic wastewater COD and other water quality changes exhibit a similar trend. The simulated wastewater COD reduction is estimated to be in the range of 94-136, with the aerobic tanks reducing by 131-151, the anaerobic tanks by 292-332, and the secondary sedimentation tanks by 5-37. Similarly, the quality of the COD in aerobic and anaerobic tanks exhibits comparable alterations, as illustrated in the figure. The gradual reduction of COD can be attributed to the

Table 3: Results of phosphorus remover dosing at different stages with simulated domestic wastewater.

	Aerobic Tanks	Anaerobic Tanks	Secondary Sedimentation Tanks	Simulated Domestic Wastewater
PH	7.2	7	7.1	7
ORP	88	-80	10	64.5
ZATA	-10.5	-20	-17	-10.5
COD	189	358	52	400
Phosphorus Concentration	7	11.8	13.7	10.5

Table 4: Water quality in aerobic tanks after dosing.

Aerobic Tanks	Iron/Phosphorus Molar Ratio	0.67	1.33	1.67	2.00	2.67
	PH	6.7	6.7	6.7	6.7	6.8
	ORP	102.8	104.5	106.3	105.9	107.4
	COD	58	52	47	44	38
	ZATA	-14	-14.5	-16.5	-16.4	-18.9
	Phosphorus Removal Rate	23.5%	52.9%	61.8%	69.1%	92.6%

Table 5: Water quality of the secondary sedimentation tank after the addition of chemicals.

Secondary Sedimentation Tanks	Phosphorus Concentration	0.34	0.68	0.85	1.02	1.36	1.70
	PH	7.2	7.1	7.2	6.8	6.8	6.8
	ORP	161.6	165.6	163	165.6	169.8	169.1
	COD	50	45	43	38	32	15
	ZATA	-21.7	-19.6	-20.1	-22.4	-18.7	-21.9
	Phosphorus Removal Rate	18.2%	32.8%	52.6%	57.7%	73.0%	81.8%

Table 6: Water quality in anaerobic tank after dosing.

Anaerobic Tanks	Phosphorus Concentration	0.40	0.79	0.99	1.19	1.58	1.97
	PH	6.9	6.9	6.8	6.8	6.8	6.8
	ORP	4.8	8	11.4	15.3	21.4	29.5
	COD	66	60	55	54	49	35
	ZATA	-14	-15.4	-17.5	-16	-17.4	-14
	Phosphorus Removal Rate	3.4%	16.1%	27.1%	39.8%	66.9%	80.5%

Table 7: Water quality of simulated effluent after dosing.

Simulated Domestic Wastewater	Phosphorus Concentration	0.43	0.85	1.06	1.27	1.70	2.12
	PH	6.3	6.2	6.1	6	5.8	5.8
	ORP	409	446.7	458.4	475.4	511.6	533
	COD	180	82	54	44	32	27
	ZATA	-17.5	-12.3	16.9	-16	-16.3	-16.1
	Phosphorus Removal Rate	34.5%	56.3%	66.3%	78.2%	93.1%	100.0%

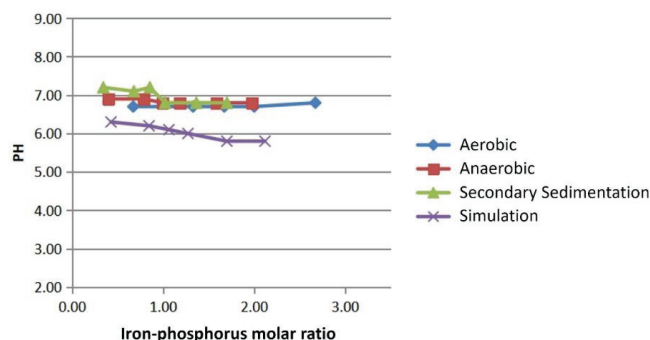


Figure 2: Influence of different water quality on pH under different ratio of Fe:P Ratio.

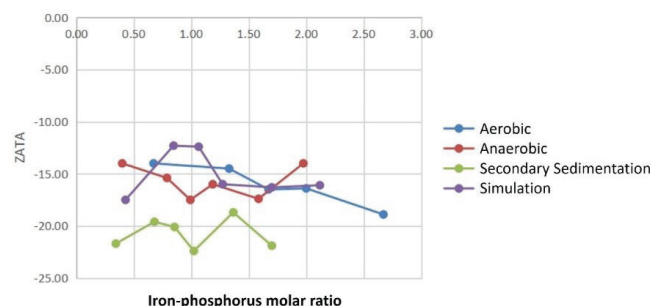


Figure 3: Influence of different water quality on ZATA under different ratio of Fe:P Ratio.

removal of iron, phosphorus, and organic matter during the process. The anaerobic tank is the most effective at removing phosphorus, yet it also has the lowest efficiency in removing

phosphorus. This is due to the organic matter impeding the removal of phosphorus. A comparison of the organic changes and phosphorus removal rate in the aerobic tank and anaerobic tank can be seen in the following figure. It can be observed that the removal of organic matter has a poor effect on the removal of phosphorus. Alternatively, it can be shown that the anaerobic tank is an effective method for removing phosphorus when combined with sedimentation. A comparison of the secondary sedimentation tank and the simulated wastewater revealed that the efficiency of organic matter removal and phosphorus removal in the simulated wastewater differed. This suggests that the various types of organic matter exert varying effects on phosphorus removal (Figure 5).

The aforementioned figure and Table 2.1 can be obtained when the dosage of iron salt and phosphorus in the water is increased. In this case, the water redox potential increases, water oxidation is accelerated, and the redox potential of the water quality presents a clear stratified distribution. The specific results for the simulation of sewage, two-sedimentation of sewage, aerobic wastewater, anaerobic wastewater, and anaerobic wastewater are presented below. This differs from the previous scenario, in which the aerobic wastewater was subjected to two sedimentation tanks prior to phosphorus removal. Moreover, the size of the ORP after dosing and the efficiency of phosphorus removal exhibited a positive correlation (Figure 6).

This Figure above illustrates the disparate impact of varying water quality on phosphorus removal. The simulation depicts the highest removal rate of sewage, followed by two sinks, aerobic and anaerobic, which exhibit the lowest performance. The figure also demonstrates that the iron and phosphorus ratio of aerobic sewage removal rate is greater than that of anaerobic sewage when the mole ratio is greater than 1.5. However, after the removal of the effect, the performance is essentially similar.

In conclusion, the analysis indicates that:

1. The initial pH of the water is 7–7.2, which demonstrates that the effect of phosphorus removal is not significant. However, the addition of phosphorus removal chemicals to simulated domestic wastewater resulted in the greatest reduction in pH value, indicating that the water quality was the most affected.

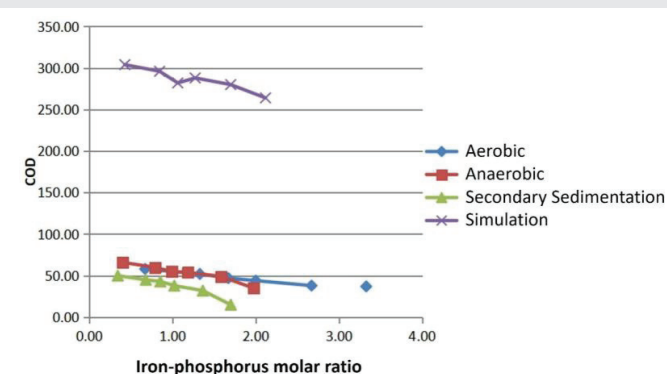


Figure 4: Influence of different water quality on COD under different ratio of Fe:P Ratio.

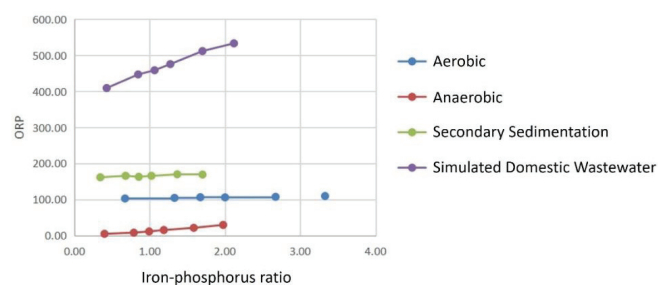


Figure 5: Influence of different water quality on ORP under different ratio of Fe:P Ratio.

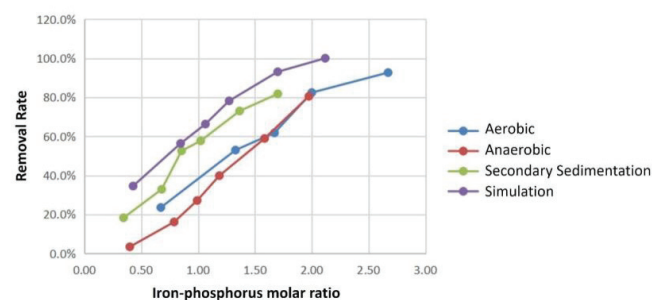


Figure 6: Influence of different water quality on Phosphate removal rate under different ratio of Fe:P Ratio.

2. A notable aspect of the study is the absence of a discernible pattern in the ZATA potential in phosphorus removal, both before and after the addition of phosphorus removal chemicals.
3. The process of phosphorus removal is accompanied by the removal of organic matter, which is a crucial finding.
4. There is a positive correlation between the solution ORP and the removal rate of phosphorus after the addition of a phosphorus removal agent. With the increase in dose, the redox potential becomes larger, indicating an enhanced oxidizing effect.

Mechanism of organics affecting on the Fe(III)-dependent phosphorus removal

Ferric ion-dependent phosphorus removal process with CA:

The mechanism of phosphorus removal by Fe(III) is currently a topic of debate and research. Two potential mechanisms of Fe(III)-dependent phosphorus removal are widely accepted: 1) Fe(III) rapidly hydrolyzes to form iron hydroxyl oxide (Fe-HFO) (Eq. 1), which then absorbs phosphate to remove phosphorus from wastewater. 2) Ferrous iron (Fe(II)) reacts directly with phosphate to form iron phosphate precipitation (Eq. 2), which is a mechanism for the removal of phosphorus [38].



The Fe-HFO then absorbs phosphate ions from the wastewater, effectively removing phosphorus. This process relies on the adsorption of phosphate to the Fe-HFO surface, which binds phosphate ions, leading to their removal from the water. This mechanism is widely considered an efficient

method for phosphorus removal, as iron hydroxide is highly effective in adsorbing phosphate under certain conditions.

Formation of Iron Phosphate Precipitation (Fe(II)-Phosphate): Another proposed mechanism is based on the reduction of Fe(III) to Fe(II), which then reacts with phosphate to form insoluble iron phosphate precipitates. The chemical equation for this reaction is:



In this mechanism, ferrous iron (Fe(II)) reacts directly with phosphate ions, forming iron phosphate (FePO_4) precipitates. These precipitates are insoluble and thus effectively remove phosphate from the aqueous phase. This mechanism typically requires the presence of reducing conditions or a source of Fe(II), which may be generated through the reduction of Fe(III) under certain environmental conditions. Both mechanisms are important in the context of Fe(III)-dependent phosphorus removal, and the relative contributions of each may depend on factors such as pH, the presence of other ions, and the specific iron species involved. The actual process may involve both mechanisms to varying extents, and ongoing research aims to better understand how these processes occur under different wastewater treatment conditions.

To investigate the mechanism through which organic compounds influence Fe(III)-dependent phosphorus removal, citric acid (CA) was selected as the representative organic compound. Two experimental groups, namely the CCPR and HFO groups, were established for this purpose. The results, as shown in Figure 7, reveal that CA had a significant effect on the efficiency of phosphorus removal in both groups. As the concentration of CA in the reaction system increased, a continuous decline in phosphorus removal efficiency was observed. Notably, when the concentration of CA was below $30 \text{ mg} \cdot \text{L}^{-1}$, the phosphorus removal efficiency in the CCPR group was higher than that in the HFO group.

In accordance with the principles of thermodynamics and the findings of Rose, et al., the hydrolysis of Fe (III) ions in aqueous solution occurs at an exceedingly rapid rate, resulting in the formation of Fe-HFO [39,40]. Figure 8 illustrates the alteration in the bulk liquid of a conventional chemical phosphorus removal system following the addition of a specific quantity of CA. Figure 8-A illustrates the formation of iron-phosphorus precipitates in the CCPR system, with a phosphorus removal percentage of 82.5%. As illustrated in Figure 8-B, following the introduction of CA into the system, the iron-phosphorus precipitate gradually diminished, and the liquid assumed a clarified, bright yellow hue. The percentage of phosphate removed was found to be zero. The precipitation of iron and phosphorus was found to be completely absent when the concentration of CA in the system reached $30 \text{ mg} \cdot \text{L}^{-1}$.

As illustrated in Figure 9, when the concentration of CA was set to zero, the phosphorus removal percentage in the CCPR group reached 86%, while the corresponding figure for the HFO group was 62.4%. It is evident that in the Fe(III)-dependent phosphorus removal process, the majority of the phosphate was removed through adsorption to the Fe-HFO

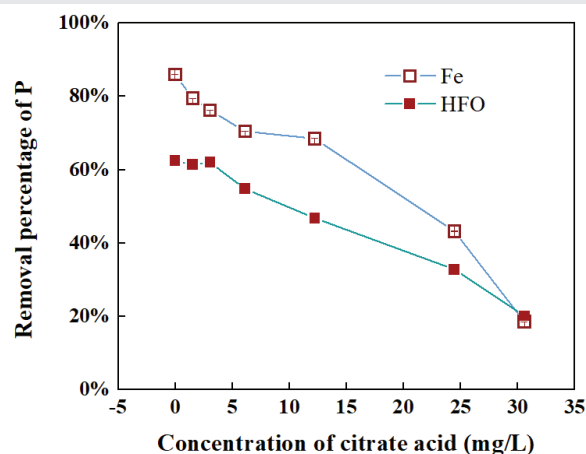


Figure 7: Effects of CA on the phosphorus removal efficiency in both CCPR group and HFO group.

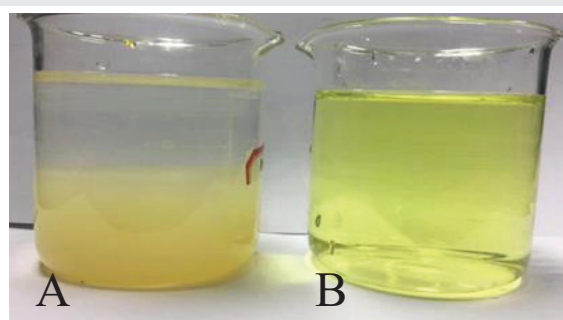


Figure 8: Effects of CA on the conventional phosphorus removal.

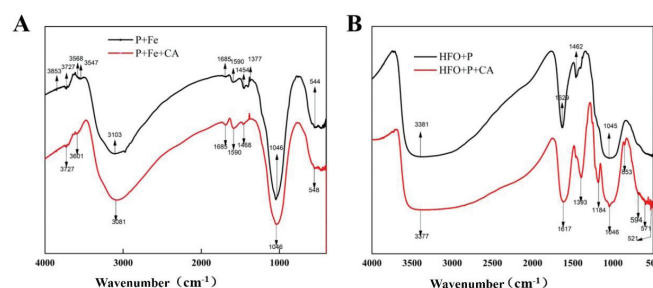


Figure 9: Fourier infrared spectrum of samples in the conventional phosphorus removal system (A) and the HFO-dependent phosphorus removal system (B).

surface. In the CCPR process, the Fe(III) was added and partially reacted directly with phosphate, forming an iron-phosphorus precipitate. The remainder of the added Fe(III) underwent hydrolysis to form Fe-HFO, which then adsorbed phosphate, thereby achieving phosphorus removal. The data demonstrated that the Fe-HFO process was responsible for 73% of the total phosphorus removal. Figure 8 illustrates the addition of CA to a system wherein an iron-phosphorus precipitate had already formed. The CA effectively displaces the HFO from the iron-phosphorus precipitate, preventing it from undergoing a complexation reaction [41], and thus preventing the formation of precipitates.

Chemical bond change in the process of Fe(III)-dependent phosphorus removal: To gain further insight into the mechanism by which organics influence Fe(III)-dependent

phosphorus removal efficiency, the formation and fracture of chemical bonds in the reaction system were analyzed using FTIR.

Figure 9-A illustrates the alteration in chemical bonds in the samples prior to and following the incorporation of CA into the CCPR group. The stretching vibration peaks of the hydroxyl group, observed at 3547 cm^{-1} and 1377 cm^{-1} , are reported in [42-44]. The addition of CA resulted in the disappearance of the peak positions at 3547 cm^{-1} and 1377 cm^{-1} , as well as a reduction in the peak areas at 3103 cm^{-1} , 1453 cm^{-1} , 1046 cm^{-1} , and others. These observations indicate that the addition of CA has affected the formation of the hydroxyl group (the number of hydroxyl groups decreased). Concurrently, the absorption band at 3103 cm^{-1} exhibited a forward shift, indicative of enhanced stability in the formation of hydrogen bonds between the novel molecules.

A thermodynamic analysis indicates that the equilibrium constant for organic ligands is predominantly greater than that of inorganic ligands. It was therefore postulated that new organic complexes may have been formed in the reaction system. In the absence of any previous reports concerning CA-phosphate complexes, it can be inferred that the newly formed organic complex within the system is a complex of CA and Fe (III).

Figure 9-B illustrates the alteration in chemical bonds in the samples prior to and following the introduction of CA into the HFO group. The absorption band at 3381 cm^{-1} , 1629 cm^{-1} , and 1462 cm^{-1} exhibited a downward shift, while new absorption bands emerged at 594 cm^{-1} , 571 cm^{-1} , and 521 cm^{-1} . This suggests that the hydrogen bond in the system was either enhanced or a new, stronger intermolecular bond was formed. Moreover, the absorption peak area at 3381 cm^{-1} and 1629 cm^{-1} exhibited a reduction, indicative of a decline in the number of hydroxyl groups within the system. The same result was observed in Figure 9-A, which led to the hypothesis that CA reacted with Fe-HFO to form a complex.

The addition of CA disrupted the original chemical equilibrium during the Fe(III)-dependent phosphorus removal process. The CA demonstrated a stronger affinity for the Fe-HFO than the phosphate. The addition of CA and phosphate to the system resulted in competition for the binding site of Fe-HFO, ultimately leading to the formation of an iron citrate complex. Nevertheless, the phosphate remained in solution, thereby reducing the efficiency of phosphorus removal in the system.

Product analysis of Fe(III)-dependent phosphorus removal with the CA addition: To clarify the role of citrate in modulating the Fe(III)-dependent phosphorus removal mechanism, mass balance and kinetic analyses were conducted using a centrifugal graded extraction method. Specifically, $0.22\text{ }\mu\text{m}$ membrane filtration was applied to separate dissolved and particulate fractions, $0.1\text{ mol}\cdot\text{L}^{-1}$ NaOH to desorb adsorbed phosphorus, and $1\text{ mol}\cdot\text{L}^{-1}$ HCl to dissolve precipitated phosphorus, enabling quantitative determination of phosphorus and iron speciation.

In the absence of citrate, precipitated phosphorus accounted for $65\% \pm 3\%$ of total phosphorus, with a Fe:P molar ratio of 1.02 ± 0.05 in Fe-P precipitates, indicating a precipitation-dominated mechanism. With $30\text{ mg}\cdot\text{L}^{-1}$ citrate addition, the proportion of precipitated phosphorus decreased to $18\% \pm 2\%$, while the Fe:P ratio in Fe-P precipitates increased to 2.3 ± 0.1 . Meanwhile, adsorbed phosphorus rose from $28\% \pm 2\%$ to $52\% \pm 3\%$, and the fraction of Fe associated with Fe-HFO increased from $32\% \pm 3\%$ to $67\% \pm 4\%$. Mass balance closure was achieved with deviations $<5\%$ between calculated and initial values. Kinetic monitoring further demonstrated that without citrate, precipitated phosphorus accumulated rapidly within the first 5 minutes (rate constant $0.12 \pm 0.01\text{ min}^{-1}$) and stabilized after 10 minutes. In contrast, citrate addition markedly suppressed precipitation (rate constant $0.01 \pm 0.002\text{ min}^{-1}$), while adsorbed phosphorus increased gradually with Fe-HFO formation (rate constant $0.03 \pm 0.003\text{ min}^{-1}$). These results confirm that citrate inhibits Fe-P precipitation while promoting Fe-HFO adsorption, thereby shifting the phosphorus removal pathway from precipitation-dominated to adsorption-dominated. The composition of the products in the CCPR and HFO groups was analyzed by X-ray Diffraction (XRD) before and after the addition of CA. The results are presented in Figure 10.

Figure 10-A illustrates the alteration in the composition of the CCPR group prior to and following the incorporation of CA. Prior to the addition of CA, the phosphate in the system underwent a reaction with the Fe (III) ions, resulting in the formation of iron-phosphorus crystals (as evidenced by the sharp peak observed in the P+Fe curve in Figure 10-A). The specific species are presented in Table 2. Following the addition of CA, the original crystal structure of iron and phosphorus was disrupted, and the samples were predominantly observed to exist in the form of amorphous Fe-HFO (P+Fe+CA curve in Figure 10-A, Table 2).

Figure 10-B illustrates the compositional alterations in the HFO group prior to and following the introduction of CA. No crystals were generated in the HFO system (Figure 10-B, Table 2) [45]. Upon the addition of phosphate, iron-phosphorus crystals emerged within the system (HFO+P curve in Figure 10-B, Table 2), exhibiting a spectrum analogous to that of the P+Fe curve in Figure 10-A. This observation substantiates the assertion that the HFO group represents the crux of the CCPR process. Upon the continual addition of CA to the system (HFO+P+CA curve in Figure 10-B), the sharp peak of the HFO+P curve was no longer evident (Figure 10-B), indicating that the

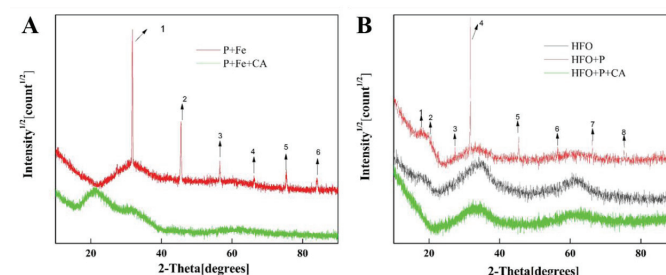


Figure 10: XRD spectrum of samples in the conventional phosphorus removal system (A) and the HFO-dependent phosphorus removal system (B).

iron-phosphorus crystal structure was destroyed and that CA had effectively “preempted” the Fe-HFO. This resulted in the release of phosphate into the solution and a reduction in the efficiency of phosphorus removal. A comparison of the P+Fe+CA curve in Figure 10-A with the HFO+P+CA curve in Figure 10-B demonstrates that the differing addition order of phosphate and Fe (III) resulted in disparate products. The addition of Fe(III) to a system containing CA and phosphate resulted in the formation of products with reduced purity. However, in a system containing Fe-HFO and phosphate, the addition of CA did not result in any alteration to the HFO species. CA is more competitive than phosphate in terms of competing for Fe-HFO, and CA affects the efficiency of phosphorus removal that is dependent on ferrous iron (Table 8).

Table 8: XRD crystal pattern analysis.

Number	Species	Formula
P+Fe		
3	Barbosalite	$\text{Fe}_3(\text{PO}_4)_2(\text{OH})_2$
2	Cyrllovite	$\text{Fe}^{2+}\text{Fe}^{3+}(\text{PO}_4)_2(\text{OH})_2$
1	Dufrenite	$\text{Fe}_3(\text{PO}_4)_3(\text{OH}) \cdot 2\text{H}_2\text{O}$
1	Iron Hydrogen Phosphate Hydrate	$\text{Fe}_3\text{H}_{15}(\text{PO}_4)_8 \cdot 4\text{H}_2\text{O}$
1	Phosphosiderite	$\text{Fe}^{3+}\text{PO}_4 \cdot 2\text{H}_2\text{O}$
2,3	Strengite	$\text{FePO}_4 \cdot 2\text{H}_2\text{O}$
2,3	Vofeite	$\text{Fe}_2\text{PO}_4(\text{OH})$
P+CA+Fe		
	Beraunite	$\text{Fe}^{2+}\text{Fe}^{5+}(\text{PO}_4)_4(\text{OH}) \cdot \text{H}_2\text{O}$
	Dufrenite	$\text{Fe}_3(\text{PO}_4)_3(\text{OH}) \cdot 2\text{H}_2\text{O}$
	Iron Hydrogen Phosphate Hydrate	$\text{H}_3\text{Fe}(\text{PO}_4)_2 \cdot 2.5\text{H}_2\text{O}$
	Iron Hydrogen Phosphate Hydrate	$\text{FeH}_2\text{P}_3\text{O}_{10} \cdot 1.5\text{H}_2\text{O}$
	Ludlamite	$\text{Fe}_3(\text{PO}_4)_2 \cdot 4\text{H}_2\text{O}$
	Whitmoreite	$\text{FeFe}_2(\text{PO}_4)_2(\text{OH}) \cdot 4\text{H}_2\text{O}$
HFO		
	Akaganeite	$\text{Fe}_3\text{O} \cdot \text{H}_2\text{O}$
	Feroxyhyte	$\text{Fe}^{3+}\text{O}(\text{OH})$
	Ferrihydrite	$\text{Fe}_5\text{O}_7(\text{OH})$
	Gothite	$\text{Fe}_2\text{O}_3/\text{Fe}_2\text{O}_3 \cdot \text{H}_2\text{O}/\text{Fe}^{3+}\text{O}(\text{OH})$
	Hydrohematite	$\text{Fe}_2\text{O}_3 \cdot n\text{H}_2\text{O}$
	Iron Hydroxide	$\text{Fe}(\text{OH})_2/\text{Fe}(\text{OH})_3$
	Iron Oxide Hydroxide	$\text{FeOOH}/\text{Fe}_2\text{O}_3 \cdot \text{H}_2\text{O}/\text{FeO}(\text{OH})$
	Lepidocrocite	$\text{Fe}_2\text{O}_3 \cdot \text{H}_2\text{O}/\text{Fe}^{3+}\text{O}(\text{OH})$
HFO+P		
1	Iron Hydrogen Phosphate	$\text{FeH}_2\text{P}_2\text{O}_7$
	Hydromolysie	$\text{FeCl}_3 \cdot 6\text{H}_2\text{O}$
2	Hydromolysie	$\text{FeCl}_3 \cdot 6\text{H}_2\text{O}$
	Vivianite	$\text{Fe}_3(\text{PO}_4)_2 \cdot 8\text{H}_2\text{O}$
3	Iron Hydrogen Phosphate	$\text{FeH}_2\text{P}_2\text{O}_7$
	Iron Hydrogen Phosphate	$\text{FeH}_{2/3}\text{P}_3\text{O}_{10}$
	Iron Hydrogen Phosphate Hydrate	$\text{FeH}_2\text{P}_3\text{O}_{10} \cdot \text{H}_2\text{O}$
	Iron Hydrogen Phosphate Hydrate	$\text{H}_3\text{Fe}(\text{PO}_4)_2 \cdot 5\text{H}_2\text{O}$
4	Iron Hydrogen Phosphate	$\text{FeH}_2\text{P}_3\text{O}_{10}$
	Iron Hydrogen Phosphate Hydrate	$\text{H}_3\text{Fe}(\text{PO}_4)_2 \cdot 2.5\text{H}_2\text{O}$
5	Strengite	$\text{FePO}_4 \cdot 2\text{H}_2\text{O}$
	Iron Hydrogen Phosphate	$\text{FeH}_2\text{P}_2\text{O}_7$
6	Iron Hydrogen Phosphate	$\text{FeH}_3(\text{PO}_4)_2 \cdot 4\text{H}_2\text{O}$
	Iron Hydrogen Phosphate Hydrate	$\text{H}_3\text{Fe}(\text{PO}_4)_2 \cdot 2.5\text{H}_2\text{O}$
7,8	Lepidocrocite	$\text{Fe}^{3+}\text{O}(\text{OH})$
HFO+CA+P		
	Devauite	$\text{Fe}_3(\text{PO}_4)_3(\text{OH}) \cdot 3\text{H}_2\text{O}$
	Iron Hydrogen Phosphate	$\text{Fe}(\text{H}_2\text{PO}_4)_3$
	Iron Hydrogen Phosphate Hydrate	$\text{FeH}_3\text{P}_2\text{O}_4 \cdot 3\text{H}_2\text{O}$
	Ludlamite	$\text{Fe}_3(\text{PO}_4)_2 \cdot 4\text{H}_2\text{O}$

Mechanism of the effect of CA on Fe(III)-dependent phosphorus removal efficiency: The fundamental principle underlying the CCPR group process is the adsorption and precipitation of phosphate by the Fe-HFO. As illustrated in Figure 11-A, when the pH value is above 2.2 in the bulk liquid, the Fe (III) undergoes hydrolysis upon entering the water body, resulting in the formation of the Fe-HFO. The Fe-HFO adsorbs the phosphate, forming precipitates that achieve the objective of phosphorus removal.

Figure 11-B illustrates the mechanism of the ferrous iron-dependent phosphorus removal process in the absence of CA. In the aqueous environment, the predominant form of Fe(III) is the HFO. The phosphate is absorbed by the HFO, forming flocs which subsequently precipitate. Only a limited number of dissolved ferric ions undergo a reaction with phosphate to form Fe-P precipitates [46].

Figure 11-C illustrates the mechanism of the Fe-HFO process in the presence of CA. In the presence of CA in the water body, the Fe (III) initially undergoes hydrolysis to form Fe-HFO. In comparison to phosphates, the CA exhibits a greater affinity for the Fe-HFO, occupying the adsorption site and displacing the phosphate. Additionally, the CA forms a complex with free Fe(III) ions, namely iron citrate, which also reduces the efficiency of phosphorus removal in the system.

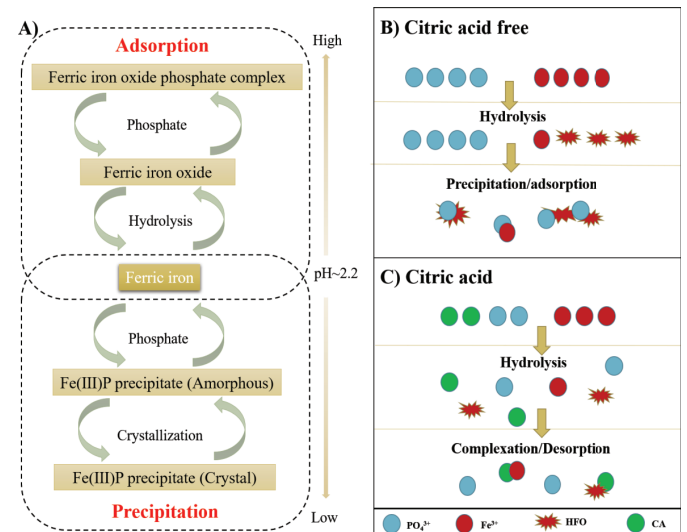


Figure 11: Mechanism of the effect of CA on ferrous iron-dependent phosphorus removal efficiency.

Conclusion

This study systematically elucidated the inhibitory effects of organics on Fe(III)-mediated phosphorus removal. Results confirm that carboxyl-rich compounds, particularly polycarboxylic acids, exert disproportionately strong interference by competing for Fe-hydroxide surface sites and forming stable Fe-organic complexes. Consequently, adsorption onto Fe-hydroxide remains the dominant removal pathway, while direct precipitation contributes less. The key findings are summarized as follows:

- 1. Influence of organic functional groups:** Carboxyl-containing organics exhibited a significantly greater inhibitory effect on phosphorus removal compared to hydroxyl-containing organics under Fe(III)-mediated conditions.
- 2. Dominant removal pathway:** The conventional Fe(III)-dependent phosphorus removal mechanism is primarily driven by the adsorption of phosphate onto Fe-hydroxide flocs (Fe-HFO), which accounted for approximately 73% of total phosphorus removal. In contrast, direct precipitation via chemical complexation with free Fe(III) contributed only 27%.
- 3. Mechanistic insight:** The reduced phosphorus removal efficiency in the presence of carboxyl organics is attributed to competitive binding. Carboxyl groups preferentially occupy the active sites on Fe-HFO, thereby inhibiting phosphate adsorption and disrupting the Fe-P precipitation pathway.
- 4. Engineering implications:** Pre-removal of carboxyl-functional organics may enhance the efficiency of Fe(III)-based phosphorus removal systems. This finding offers a promising strategy for optimizing future wastewater treatment processes.

From an engineering perspective, these findings highlight that wastewater with high VFA/DOC ratios or elevated carboxyl fractions poses a significant challenge to chemical phosphorus removal. Practical strategies include pretreatment to reduce carboxyl organics, adaptive Fe(III) dosing, and pH optimization to balance Fe-hydrolysis and minimize complex stability. While laboratory-scale experiments provided clear mechanistic insights, real wastewater systems are more complex, with variable ionic strength, alkalinity, and organic diversity. Thus, future work should focus on validating these mechanisms in pilot or full-scale systems, refining pretreatment technologies, and developing advanced Fe-based or hybrid materials with higher selectivity and resilience against organic interference.

Overall, the study establishes a quantitative and mechanistic basis for improving Fe(III)-based phosphorus removal under organic-rich conditions, offering actionable guidance for wastewater treatment plants while pointing toward the need for more robust, adaptive treatment strategies.

Supplementary materials: Supplementary material associated with this article can be found.

Author contributions: Lu Xincheng: Writing-original draft, original draft, methodology, investigation. Zhao Zhiguo: methodology, investigation, Wang Wenyan: investigation, BAO Lei: Writing-original draft, original draft, Cao Qixin: Investigation, funding acquisition, Yang Xian, Tan Huan: Visualization, data curation, Lai Lingling: Visualization, data curation, Liu Mengyu: Visualization, data curation, Yang Fugang: Visualization, data curation, Li Yong: Visualization, data curation, Li Diandian: Visualization, data curation. All authors have read and agreed to the published version of the manuscript.

Acknowledgement

We gratefully acknowledge the support of National Natural Science Foundation of China (51278406) and National Youth Science Foundation of China (51808433).

Institutional review board statement

Informed Consent Statement: Informed consent was obtained from all subjects involved in the study.

Data Availability Statement: All individuals included in this section have consented to the acknowledgement.

Acknowledgment: The authors would like to thank the Tianjin University for providing experimental facilities and technical support.

References

- Yu N, Yuan L, Lü J. Characteristics of chemical phosphorus precipitation of wastewaters from a municipal wastewater treatment plant and its influencing factors. *Chin J Environ Eng*. 2015;9(12):5813–5817.
- Lacasa E, Cañizares P, Sáez C, Fernández FJ, Rodrigo MA. Electrochemical phosphates removal using iron and aluminum electrodes. *Chem Eng J*. 2011;172:137–143. Available from: <https://doi.org/10.1016/j.cej.2011.05.080>
- Fytianos K, Raikos N, Voudrias E. Modeling of phosphorous removal from aqueous and wastewater samples using ferric iron. *Environ Pollut*. 1998;101(1):123–130. Available from: [https://doi.org/10.1016/S0269-7491\(98\)00007-4](https://doi.org/10.1016/S0269-7491(98)00007-4)
- Marguti AL, Ferreira Filho SS, Piveli RP. Physical-chemical process optimization for phosphorus removal from domestic wastewater by chemical precipitation with ferric chloride. *Eng Sanit Ambient*. 2008;13:395–404. Available from: https://www.researchgate.net/publication/262509212_Physical-chemical_process_optimization_for_phosphorus_removal_from_domestic_wastewater_by_chemical_precipitation_with_ferric_chloride
- Thistleton J, Berry TA, Pearce P, Parsons SA. Mechanisms of chemical phosphorus removal II—iron(III) salts. *Process Saf Environ Prot*. 2002;80:265–269. Available from: https://ui.adsabs.harvard.edu/link_gateway/2002PSEP...80..265T/doi:10.1205/095758202762277623
- Sisk L, Benefield L, Reed B. Ortho-phosphate removal from a synthetic wastewater using lime, alum, and ferric-chloride. *Sep Sci Technol*. 1987;22:1471–1501. Available from: <https://doi.org/10.1080/01496398708058412>
- Luedecke C, Hermanowicz SW, Jenkins D. Precipitation of ferric phosphate in activated-sludge—a chemical-model and its verification. *Water Sci Technol*. 1989;21:325–337. Available from: https://ui.adsabs.harvard.edu/link_gateway/1989WSTec...21..325L/doi:10.2166/wst.1989.0235
- Zhang T, Ding LL, Ren HQ, Guo ZT, Tan J. Thermodynamic modeling of ferric phosphate precipitation for phosphorus removal and recovery from wastewater. *J Hazard Mater*. 2010;176:444–450. Available from: <https://doi.org/10.1016/j.jhazmat.2009.11.049>
- Takacs I, Murthy S, Fairlamb PM. Chemical phosphorus removal model based on equilibrium chemistry. *Water Sci Technol*. 2005;52:549–555. Available from: <https://pubmed.ncbi.nlm.nih.gov/16459833/>
- Galarneau E, Gehr R. Phosphorus removal from wastewaters: experimental and theoretical support for alternative mechanisms. *Water Res*. 1997;31:328–338. Available from: [https://doi.org/10.1016/S0043-1354\(96\)00256-4](https://doi.org/10.1016/S0043-1354(96)00256-4)

11. Smith S, Takacs I, Murthy S, Daigger GT, Szabo A. Phosphate complexation model and its implications for chemical phosphorus removal. *Water Environ Res.* 2008;80(5):428–438. Available from: <https://pubmed.ncbi.nlm.nih.gov/18605382/>
12. Hauduc H, Takács I, Smith S, Szabo A, Murthy S, Daigger GT, et al. A dynamic physicochemical model for chemical phosphorus removal. *Water Res.* 2015;73:157–170. Available from: <https://doi.org/10.1016/j.watres.2014.12.053>
13. Antelo J, Avena M, Fiol S, Lopez R, Arce F. Effects of pH and ionic strength on the adsorption of phosphate and arsenate at the goethite–water interface. *J Colloid Interface Sci.* 2005;285(2):476–486. Available from: <https://doi.org/10.1016/j.jcis.2004.12.032>
14. Pham AN, Rose AL, Feitz AJ, Waite TD. Kinetics of Fe(III) precipitation in aqueous solutions at pH 6.0–9.5 and 25°C. *Geochim Cosmochim Acta.* 2006;70:640–650. Available from: https://repository.geologyscience.ru/bitstream/handle/123456789/44884/Pham_06.pdf?sequence=1
15. Hauduc H, Takács I, Smith S, Szabo A, Murthy S, Daigger GT, et al. A dynamic physicochemical model for chemical phosphorus removal. *Water Res.* 2015;73:157–170. Available from: <https://doi.org/10.1016/j.watres.2014.12.053>
16. Nguyen DD, Ngo HH, Guo W, Nguyen TT, Chang SW, Jang A, et al. Can electrocoagulation process be an appropriate technology for phosphorus removal from municipal wastewater? *Sci Total Environ.* 2016;563–564:549–556. Available from: <https://doi.org/10.1016/j.scitotenv.2016.04.045>
17. Tran N, Drogui P, Blais JF, Mercier G. Phosphorous removal from spiked municipal wastewater using either electrochemical coagulation or chemical coagulation as tertiary treatment. *Sep Purif Technol.* 2012;95:16–25. Available from: <https://doi.org/10.1016/j.seppur.2012.04.014>
18. Zhou YN, Xing XH, Liu ZH, Cui LW, Yu AF, Feng Q, et al. Enhanced coagulation of ferric chloride aided by tannic acid for phosphorous removal from wastewater. *Chemosphere.* 2008;72(2):290–298. Available from: <https://doi.org/10.1016/j.chemosphere.2008.02.028>
19. Zhang J, Bligh MW, Liang P, Waite TD, Huang X. Phosphorus removal by in situ generated Fe(II): Efficacy, kinetics and mechanism. *Water Res.* 2018;136:120–130. Available from: <https://doi.org/10.1016/j.watres.2018.02.049>
20. Zheng X, Jin M, Zhou X, Chen W, Lu D, Zhang Y, et al. Enhanced removal mechanism of iron carbon micro-electrolysis constructed wetland on C, N, and P in salty permitted effluent of wastewater treatment plant. *Sci Total Environ.* 2019;649:21–30. Available from: <https://doi.org/10.1016/j.scitotenv.2018.08.195>
21. Guo X, Miao Y, Ge J, Cui H, Yang C, Dang Z. The influence of pH and ionic strength on the sorption of sulfamethazine by goethite. *Acta Sci Circumstantiae.* 2016;36(7):2476–2482.
22. Wu Z, Liu H, Zhang H. Research progress on mechanisms about the effect of ionic strength on adsorption. *Environ Chem.* 2010;29(6):997–1003.
23. Han Q. Global citric acid industry. *Fine Spec Chem.*
24. Tao E, Yang S, Ma H, Yu J, Jia W, Ma X. Precipitation effect of citric acid on trivalent chromium in tanning wastewater. *China Leather.*
25. Borggaard OK. Dissolution and adsorption properties of soil iron oxides. DSc Thesis. Copenhagen: DSR Forlag; 1990. Available from: https://books.google.co.in/books/about/Dissolution_and_Adsorption_Properties_of.html?id=QfpHAAAYAAJ&redir_esc=y
26. Mahasti NN, Shih YJ, Huang YH. Removal of iron as oxyhydroxide (FeOOH) from aqueous solution by fluidized-bed homogeneous crystallization. *J Taiwan Inst Chem Eng.* 2019;96:496–502. Available from: <https://doi.org/10.1016/j.jtice.2018.12.022>
27. Hiemstra T, Van Riemsdijk WH. Surface structural ion-adsorption modeling of competitive binding of oxyanions by metal (hydr)oxides. *J Colloid Interface Sci.* 1999;210:182–193. Available from: <https://doi.org/10.1006/jcis.1998.5904>
28. Liu F, He J, Colombo C, Violante A. Competitive adsorption of sulfate and oxalate on goethite in the absence and presence of phosphate. *Soil Sci.* 1999;164(3):180–189. Available from: https://journals.lww.com/soilsci/abstract/1999/03000/competitive_adsorption_of_sulfate_and_oxalate_on.4.aspx
29. Geelhoed JS, Hiemstra T, Van Riemsdijk WH. Competitive interaction between phosphate and citrate on goethite. *Environ Sci Technol.* 1998;32(14):2119–2123. Available from: <http://lib3.dss.go.th/fulltext/Journal/Environ%20Sci.%20Technology1998-2001/1998/no.14/14,1998%20vol.32,no.14,p2119-2123.pdf>
30. Sibanda H, Young S. Competitive adsorption of humus acids and phosphate on goethite, gibbsite and two tropical soils. *Eur J Soil Sci.* 1986;37:197–204. Available from: https://ui.adsabs.harvard.edu/link_gateway/1986EuJSS..37..197S/doi:10.1111/j.1365-2389.1986.tb00020.x
31. Hawke D, Carpenter PD, Hunter KA. Competitive adsorption of phosphate on goethite in marine electrolytes. *Environ Sci Technol.* 1989;23(2):187–191. Available from: <https://doi.org/10.1021/es00179a008>
32. Antelo J, Arce F, Avena M, Fiol S, López R, Macías F. Adsorption of a soil humic acid at the surface of goethite and its competitive interaction with phosphate. *Geoderma.* 2007;138:12–19. Available from: https://ri.conicet.gov.ar/bitstream/handle/11336/95033/CONICET_Digital_Nro.163562aa-8b1e-4f08-9b77-65cbc127ee60_A.pdf?sequence=2&isAllowed=y
33. Mbamba CK, Lindblom E, Flores-Alsina X, Tait S, Anderson S, Saagi R, et al. Plant-wide model-based analysis of iron dosage strategies for chemical phosphorus removal in wastewater treatment systems. *Water Res.* 2019;155:12–25. Available from: <https://doi.org/10.1016/j.watres.2019.01.048>
34. Yanoeng M. The mechanism and mathematical model study on the interaction between iron and phosphate in water.
35. Song J, Jia SY, Yu B, Wu SH, Han X. Formation of iron (hydr)oxides during the abiotic oxidation of Fe(II) in the presence of arsenate. *J Hazard Mater.* 2015;294:70–79. Available from: <https://doi.org/10.1016/j.jhazmat.2015.03.048>
36. Bolan NS, Naidu R, Mahimairaja S, Baskaran S. Influence of low-molecular-weight organic acids on the solubilization of phosphates. *Biol Fertil Soils.* 1994;18:311–319. Available from: <https://link.springer.com/article/10.1007/BF00570634>
37. Hue NV. Effects of organic acids/anions on P sorption and phytoavailability in soils with different mineralogies. *Soil Sci.* 1991;152(6):463–471. Available from: <http://dx.doi.org/10.1097/00010694-199112000-00009>
38. Gaume A, Weidler PG, Frossard E. Effect of maize root mucilage on phosphate adsorption and exchangeability on a synthetic ferrihydrite. *Biol Fertil Soils.* 2000;31:525–532. Available from: <https://ira.agroscope.ch/it-CH/publication/2947>
39. Rose AL, Waite TD. Kinetics of hydrolysis and precipitation of ferric iron in seawater. *Environ Sci Technol.* 2003;37(17):3897–3903. Available from: <https://doi.org/10.1021/es034102b>
40. Hauduc H, Takács I, Smith S, Szabo A, Murthy S, Daigger GT, et al. A dynamic physicochemical model for chemical phosphorus removal. *Water Res.* 2015;73:157–170. Available from: <https://doi.org/10.1016/j.watres.2014.12.053>
41. Stumm W, Huang CP, Jerkins SR. Specific chemical interactions affecting the stability of dispersed systems. *Croat Chem Acta.* 1970;42:223–224. Available from: <https://hrcak.srce.hr/index.php/en/197549>

42. Sun XH, Doner HE. An investigation of arsenate and arsenite bonding structures on goethite by FTIR. Soil Sci. 1996;161(12):865–872. Available from: <http://dx.doi.org/10.1097/00010694-199612000-00006>
43. Fendorf S, Eick MJ, Grossl P, Sparks DL. Arsenate and chromate retention mechanisms on goethite: surface structure. Environ Sci Technol. 1997;31(2):315–319. Available from: <http://dx.doi.org/10.1021/es950653t>
44. Nyquist RA, Kagel RO. Infrared Spectra of Inorganic Compounds. San Diego (CA): Academic Press; 1971. Available from: <https://www.scrip.org/>

(S(i43dyn45te-exjx455q1t3d2q))/reference/referencespapers?referenceid=1324041

45. Gotić M, Music S. Mössbauer, FT-IR and FE-SEM investigation of iron oxides precipitated from FeSO₄ solutions. J Mol Struct. 2007;834–836:445–453. Available from: <http://dx.doi.org/10.1016/j.molstruc.2006.10.059>
46. Gan H, Xu S. Adsorption and desorption of phosphorus on red soil and its organic and inorganic complexes. Chin J Soil Sci. 1994;25(6):265–268.

Discover a bigger Impact and Visibility of your article publication with Peertechz Publications

Highlights

- ❖ Signatory publisher of ORCID
- ❖ Signatory Publisher of DORA (San Francisco Declaration on Research Assessment)
- ❖ Articles archived in worlds' renowned service providers such as Portico, CNKI, AGRIS, TDNet, Base (Bielefeld University Library), CrossRef, Scilit, J-Gate etc.
- ❖ Journals indexed in ICMJE, SHERPA/ROMEO, Google Scholar etc.
- ❖ OAI-PMH (Open Archives Initiative Protocol for Metadata Harvesting)
- ❖ Dedicated Editorial Board for every journal
- ❖ Accurate and rapid peer-review process
- ❖ Increased citations of published articles through promotions
- ❖ Reduced timeline for article publication

Submit your articles and experience a new surge in publication services
<https://www.peertechzpublications.org/submission>

Peertechz journals wishes everlasting success in your every endeavours.